Long Zooplankton Time Series With High Temporal and Spatial Resolution

Gary Borstad[1], Leslie Brown[1], Mei Sato[2], David Lemon[1], Randy Kerr[1] and Peter Willis[1]

[1]ASL Environmental Sciences Inc.
#1-6703 Rajpur Place
Victoria, British Columbia, Canada V8M 1Z5

[2]University of Victoria
School of Earth and Ocean Sciences
PO Box 3065 STN CSC
Victoria, British Columbia, Canada V8W 3V6

Abstract- **Long time series of acoustic sounding data present the opportunity to examine vertical distribution and behavior of zooplankton and other organisms. In this paper, we describe a small, inexpensive, single frequency (200 kHz), upward-looking water column profiler that is mounted as part of the VENUS cabled observatory in Saanich Inlet, British Columbia, Canada, and introduce the concept of depth-time 'cubes' for thinking of long time series of acoustic data. Instrument calibration is discussed, and data are calibrated to absolute volume backscattering strength. A two-year long time series of daytime scattering measurements is presented to illustrate seasonal changes at this location. We also show that with simple algorithms and uncalibrated data at a single frequency, we can track seasonal changes in the timing of zooplankton diel vertical migration with high temporal resolution. The diel vertical migration is shown to relate very closely to sun declination as expected, but the simple algorithm used to find the timing was often confused by fish and physical water movements. A more intelligent algorithm taking advantage of the high temporal resolution of the data is required.**

I. INTRODUCTION

Ship mounted sonars have been used to detect, map and measure fish and zooplankton populations in the ocean since the 1950s and are in routine use to map distributions over relatively large areas, but they are not able to provide long time series. Self-contained echo sounders such as Acoustic Doppler Current Profilers (ADCPs), either moored at depth looking upward, or mounted on surface buoys looking downward, produce time series of acoustic backscatter that have been used since the late 1980s to monitor long-term vertical distribution and behavior of zooplankton and other populations at a single location [e.g., 1, 2]. However ADCPs are designed to measure currents, and are not optimized for measuring backscatter.

Smaller Acoustic Water Column Profilers (AWCPs) are now being manufactured specifically for measuring backscatter [3], and more than 40 have been deployed around the world for autonomous operation. They are capable of operating at very high temporal and spatial resolution: pinging rates up to 1 Hz, with spatial resolution down to 1/8 meter over depths up to 300 m. This type of data can also be obtained from the RSSI (Received Signal Strength Indicator) of an ADCP, however the AWCP has significant performance advantages when long-duration or high sampling-rate deployments are considered [4]. AWCP instruments are now also being integrated into cabled observatories to allow near real-time interrogation and monitoring of the time varying vertical distribution of scattering particles [5]. One such instrument has been operated continuously on the VENUS cabled observatory in Saanich Inlet, British Columbia, for more than four years.

Single-frequency measurements are not capable of identifying the source of the backscatter, or of separating contributions from mixed populations, but can nevertheless provide valuable information on the abundance and behavior of zooplankton populations over extended periods of time. It also is frequently not possible to differentiate echoes received from a few strong reflectors and those from a cloud of many smaller scatterers distributed through the beam. A dense cloud of euphausiids and a low density school of larger fish could look similar, however individual fish targets can often be identified by their behavior and relatively limited duration in the beam. Because the AWCP's Time Varying Gain (TVG, discussed later) is set for volume backscatter, single targets such as individual fish will appear weaker at increased range.

Although similar data can be obtained with an ADCP, the AWCP has some significant advantages in spatial and temporal

resolution when long, self-powered deployments are considered [4]. An ADCP operating in 150 m water depth, with 1 m range resolution and transmitting a 30-ping ensemble every minute, would require 3 times the battery capacity of an AWCP operating at the same depth with 0.5 m range resolution, transmitting a 3-ping group 5 times per minute. In most cases, operating the ADCP to achieve high-resolution backscatter data also degrades its performance for measuring current velocity.

II. Instrument, Data and Study Location

A. The Acoustic Water Column Profiler (AWCP) and Data

The instrument, the VENUS observatory and the study location have been previously described [3, 5], but will be briefly summarized here. The inverted echo sounder is a 200 kHz Acoustic Water Column Profiler™ (AWCP), manufactured by ASL Environmental Sciences Inc. In autonomous operation, the instrument operates on internal batteries, but in the VENUS configuration, cables to shore provide power and real-time communication. In this mode it also has no data storage since all data are immediately transmitted through the cable to the VENUS Data Management and Archive System (DMAS). The instrument ping rate is selectable. For shore powered installations a fast 1 Hz rate is normal, but for long battery powered deployments the rate can be reduced to save storage. On VENUS, the ping rate was reduced to 0.3 Hz to avoid interference from other acoustic instrumentation on the same platform. Transmissions have a source level of approximately 213 dB relative to 1μPa at 1 m distance, and while the length of the transmitted pulse can be selected from 4 to 1020 μsec, the Saanich Inlet instrument is nominally set at 300 μsec. The transducer has a 3 dB beamwidth of 8 degrees, with sidelobes at -17 dB or less. Note that the 8 degree beamwidth means that the area insonified varies between 0.2 m^2 near the transducer to nearly 140 m^2 at a distance of 100 m.

The AWCP signal is expressed as Volume Backscatter (S_v) which is a logarithmic ratio of the energy illuminating the target to the backscattered signal from the volume:

$$S_v = 10 \log (I_e/I_i)$$

where S_v is measured in decibels (dB), I_e is the backscattered echo intensity 1 m from the volume and I_i is the incident sound intensity. Because I_e is always less than I_i, S_v is always negative.

After transmission, echoes arriving at the transducer pass through a preamplifier and bandpass filter, then through a Time-Varying Gain (TVG) stage and an envelope detector to the Analog to Digital (A/D) converter. The amplitude is sampled at 23.3 kHz with 8-bit resolution to a selected maximum range of 200 m or less. The digitization rate provides range resolution of approximately 1/8 meter. The Time Varying Gain has an 80 dB range, and follows an approximate 20logR +2αR form, where α is the absorption coefficient for 200 kHz sound in sea water and R is the range. The gain at which the TVG starts can be selected from one of 4 values, to allow some adjustment of the limited dynamic range of the 8-bit A/D currently installed.

The counts, N, output by the A/D converter range between 0 and 255 and are related to the volume backscatter strength S_v at range R and Source Level SL by (1):

$$S_v = 20\log N - G(2R/c) - OCV - SL + 20\log R + 2\alpha R - 10\log(½c\tau\Psi) \qquad (1)$$

where c is the speed of sound, τ is the transmitted pulse width, Ψ is the equivalent solid angle of the transducer beam, G(2R/c) is the instrument time-varying gain function in dB, and OCV is the transducer receiving response. If the Time-Varying Gain function in the instrument exactly matches the spreading and absorption losses, equation (1) shows that the logarithm of N is directly proportional to S_v. The TVG in the VENUS AWCP is an analogue circuit, and is based on an assumed speed of sound and absorption coefficient, and therefore does not usually exactly compensate for the spreading and absorption losses. Correction for that difference is necessary to convert N to S_v. The difference varies with range and can be 6 dB or greater, depending on the difference between the actual water properties and those assumed for the TVG. Using measured values for the TVG and the manufacturer's transducer specifications reduces the deviation from direct proportionality to approximately 3 dB. The uncertainty can be further reduced by calibrating the complete instrument response with known targets.

The range in S_v detectable by the AWCP is determined by the dynamic range of the A/D conversion, the TVG selected and the internal noise level of the instrument. Increasing the overall gain lowers the maximum S_v at which the A/D saturates and amplifies weaker returns, but also amplifies instrument noise. Lowering the overall gain allows detection of stronger returns without saturation, but weaker returns will then fall below the A/D's least bit level. The VENUS AWCP in Saanich Inlet uses TVG setting 2; at 50m range it can detect returns from S_v between approximately -84 and -40 dB without saturation. At 100 m

range, those limits are -73 to -36 dB.

B. Calibration of the Acoustic Water Column Profiler

Combining bench measurements of the instrument electronic properties and the specified properties of the transducer leaves some uncertainty in the instrument calibration, as it does not account for variations in response that may arise when the components of the instrument are operating in combination rather than isolation. This can be reduced by measuring the response from a known target sphere under controlled conditions in water, which allows the overall instrument response to be measured. The calibration measures the difference (ΔTS) between the Target Strength measured *in situ* ($TS_{in\ situ}$) and the theoretical value estimated using a model (TS_{model}) for solid, homogeneous elastic spheres [6, 7, 8]. $TS_{in\ situ}$ was calculated by

$$TS_{in\ situ} = 20\log N - G(2R/c) - OCV - SL + 40\log R + 2\alpha R \qquad (2)$$

where TS is a measure of the reflectivity of the target sphere. Since it is a discrete object, it does not depend on the insonified volume, as does S_v.

In February 2010, calibration measurements of AWCP #1007 were conducted at the buoy of the Ocean Technology Test Bed (OTTB), a subsea engineering laboratory operated by the University of Victoria located in Saanich Inlet [9]. The AWCP transducer was mounted to look downward from a depth of approximately 0.5 m, and data were recorded as the instrument viewed a tungsten carbide sphere with a diameter of 38.1 mm. The position of the sphere was changed vertically and horizontally in order to find the acoustic axis. Calibration measurements were acquired with the sphere located at seven different depths. Temperature and salinity were measured by CTD to compute sound speed.

The sound speed of 1476 m s^{-1} was used to compute calibration values. During calibration runs on the acoustic axis, received signals of 171-256 acoustic transmissions were averaged to determine accurate range and backscattered intensity signals at each depth. TS_{model} was estimated to be -39.49 dB based on known parameters of tungsten carbide [7, 10] and the center frequency of the AWCP. ΔTS varied from -3.21 to -0.60 dB, depending on the depth of the calibration sphere (Table 1). Since the insonified volume increases with range, the calibration sphere is more likely to be accurately positioned on the acoustic axis at longer range. Therefore, ΔTS observed at the maximum range of 37 m was applied as a constant correction to the system gain to calculate S_v.

TABLE 1.
CALIBRATION VALUES FOR AWCP #1007.

Range (R) [m]	20logN [dB]	G(2R/c) [dB]	40logR+2αR [dB]	$TS_{in\ situ}$ [dB]	$\Delta TS = TS_{in\ situ} - TS_{model}$ [dB]
17.48	47.94	119.42	51.27	-42.21	-2.72
18.49	47.67	119.42	52.34	-41.41	-1.92
20.52	45.66	120.70	54.34	-42.70	-3.21
22.67	46.01	120.70	56.26	-40.43	-0.94
24.69	44.90	120.91	57.92	-40.09	-0.60
30.76	42.33	123.26	62.29	-40.64	-1.15
36.83	40.11	124.54	65.96	-40.47	-0.98

C. The VENUS Observatory

The VENUS cabled observatory is a permanent oceanographic research facility that came on line in February 2006 [4]. Two cabled arrays are in operation in the coastal waters of southern British Columbia on Canada's Pacific coast, one of which is deployed in Saanich Inlet (Fig. 1). The bottom-mounted instrument platforms carry a number of instruments, including CTDs, oxygen and dissolved gas sensors, transmissometers and an ADCP (at times), as well as AWCPs. Other systems connected to the observatory include pan and tilt digital cameras, and a hydrophone array for monitoring ambient sounds and marine mammal communications. Real-time data are transmitted over the cable to the shore station, and thence to the University of Victoria campus. Echograms showing the last 24 hours of data and selected other days (color-coded to show N in dB as a function of range and time) are available on the VENUS website (www.venus.uvic.ca) as full day plots and as individual hourly plots. Historical data can also be obtained.
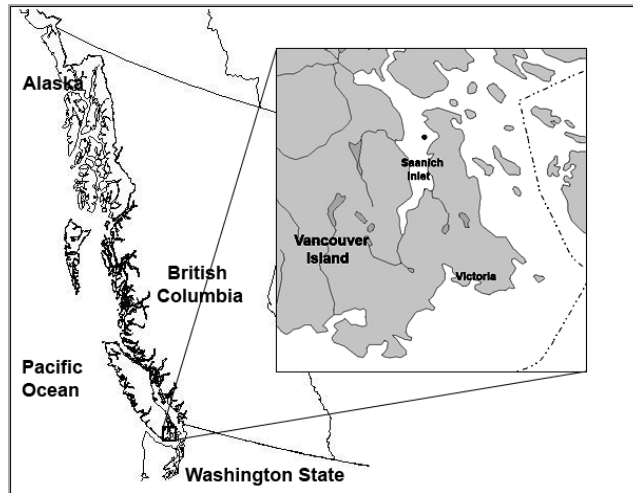
Fig. 1. Saanich Inlet, on southern Vancouver Island, British Columbia, Canada. Symbol marks the location of the VENUS Saanich Inlet observatory.

In this paper, we show examples of 200 kHz data from a single frequency AWCP installed at 96 m depth in Saanich Inlet (Fig. 1) for the period June 2008 through May 2010. An AWCP instrument has been continuously operating at this location since February 2006, with only short interruptions for maintenance and failures in other parts of the VENUS system.

D. The Study Location: Saanich Inlet, British Columbia

Saanich Inlet is a temperate fjord in the coastal waters of southern British Columbia, on the Pacific coast of Canada. A shallow (75 m) sill at the northern mouth of the inlet restricts deepwater exchange to the 230 m deep basin, and inlet waters deeper than about 80 m exhibit less than about 1mL L^{-1} dissolved oxygen. The upper extent of the anoxic (< 0.1 mL O_2 L^{-1}) layer varies between 100 and 130 m, with deep water renewal typically occurring in the autumn [11].

Primary production in Saanich Inlet is high, with a large spring phytoplankton bloom in April and May and several smaller blooms driven by wind-induced mixing during the summer and fall [12]. The inlet is home to large populations of euphausiids (*Euphausia pacifica*) that dominate the low diversity macrozooplankton community and exhibit a Diel Vertical Migration (DVM) from deep water to the surface [13, 14, 15]. These relatively large animals cause a dramatic acoustic scattering layer in the 200 kHz VENUS AWCP profiles.

The inlet is also home to abundant Pacific Herring (*Clupea pallasi*), Pacific Hake (*Merluccius productus*), and Walleye Pollock (*Theragra chalcogramma*), that feed on both juvenile and adult euphausiids [13]. Both individual fish targets and fish schools appear in the high temporal resolution AWCP data as high intensity returns (Fig. 2). Their vertical motion and speed through the sonar beam can be inferred from the orientation and horizontal length of their echo traces with time.

III. METHODS

AWCP data are provided by the VENUS Data Management and Archive System as ASCII text or as XML files. We reformatted the text files to binary and used the commercial image processing software ENVI™ from ITT for visualization and analysis. Sampled at 3 second time intervals, and in 13.2 cm vertical depth bins, 5 months of 8-bit AWCP data is a 3.5 Gigabyte file. Working with this large dataset can be a challenge: it is impossible, for example, to view the entire dataset at full resolution. We have found that it helps to think of the AWCP data as a 'cube' of [depth] x [time of day] x [days] (Fig. 2), and one can imagine 'slicing' the three-dimensional data cube in different ways. In the data cube in Fig. 2, each day begins at 00:00 GMT (16:00 PST), and the data are averaged at 1 minute intervals. The first day in the time series shown is February 28, 2009, and the last day is July 31, 2009. In this presentation, the cube has been cropped at approximately 3m, to eliminate the surface return and to expose the calendar variation in the ascent and descent timing (shown by the hourglass shape on the top surface of the cube).
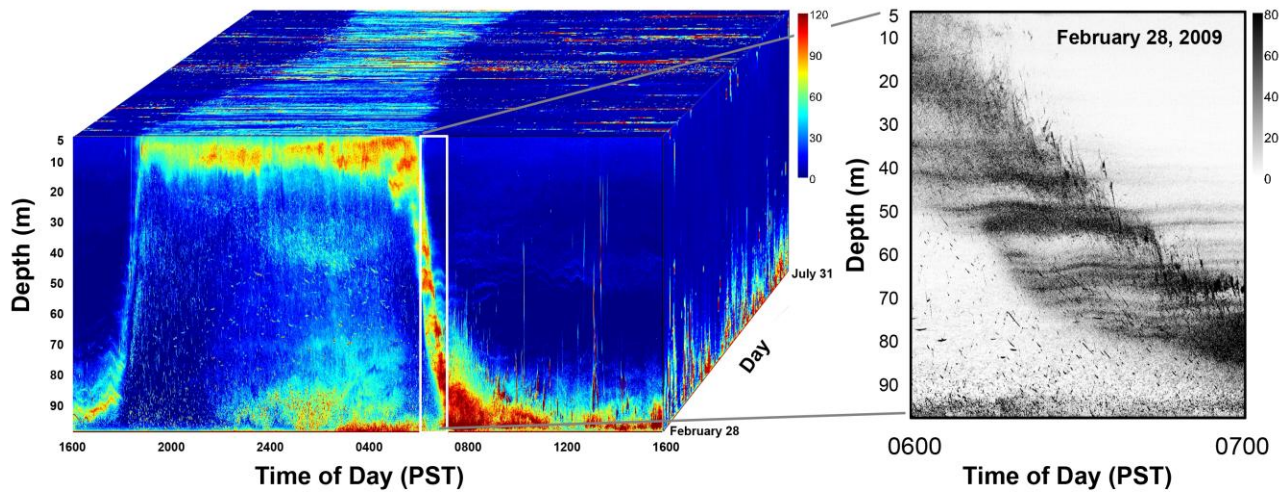
Fig. 2. Six months of uncalibrated AWCP data (but with approximate Time Varying Gain correction) shown as a 'cube', in which acoustic profiles for each day are averaged in blocks of 1 minute and plotted with a colour lookup. Each day is conceptually arranged in a time series extending in the z dimension. The grey-scale image at right illustrates the full 3 second temporal resolution for one hour between 0600 and 0700 PST on February 28 2009, the first day of the time series.

A column of pixels on the front, daily face of the cube will show the backscattering depth profile for one particular time of day - in this case on February 28 between 06:00 and 07:00 PST. Extending this in the z dimension as a YZ plane will show variation of the vertical profile with calendar day (as in Fig. 3). Similarly, vertical slices parallel to the front face of the cube capture later days in the time series. Horizontal slices describe the calendar variation of daily events at one depth stratum (Fig. 5). These slices are relatively small subsets of the large dataset and can be exported from ENVI to Microsoft Excel, Matlab or other programs where they can be further analyzed.

Averaging the data in order to reduce the volume can sometimes be dangerous because it can oversimplify events, making misinterpretations possible. The inset in Fig. 2 is a small portion of the highest temporal resolution data for February 28, and illustrates that considerable information on the behavior of fish and zooplankton is lost in averaging. In this paper, we use black and white to illustrate un-averaged full resolution data and colour to indicate temporal averages.

IV. EXAMPLES OF LONG TIME SERIES

A. Seasonal Cycle of Daytime Vertical Profiles

S_v was calculated using a constant absorption coefficient of 0.05 dB m^{-1} and sound speed of 1482 m s^{-1}, based on the mean bottom-water temperature (8.8 °C) and salinity (30.8 psu) of 2-year records. S_v at noon (12:00 PST) was extracted from 10-min, 2-m averaged data, and those data were smoothed by taking a 5-pt running mean to present the seasonal variability (Fig. 3).

During the daytime, a relatively thick scattering layer was observed near the bottom between February and July in both 2009 and 2010 (Fig 3). This layer rose to as shallow as 70 m in February 2009 and March 2010. A weaker scattering layer with more limited vertical distribution was observed in June – September 2008 and October 2009 – February 2010. Since the AWCP is located shallower than the base of daytime scattering layer, the thickness of the scattering layer cannot be determined.
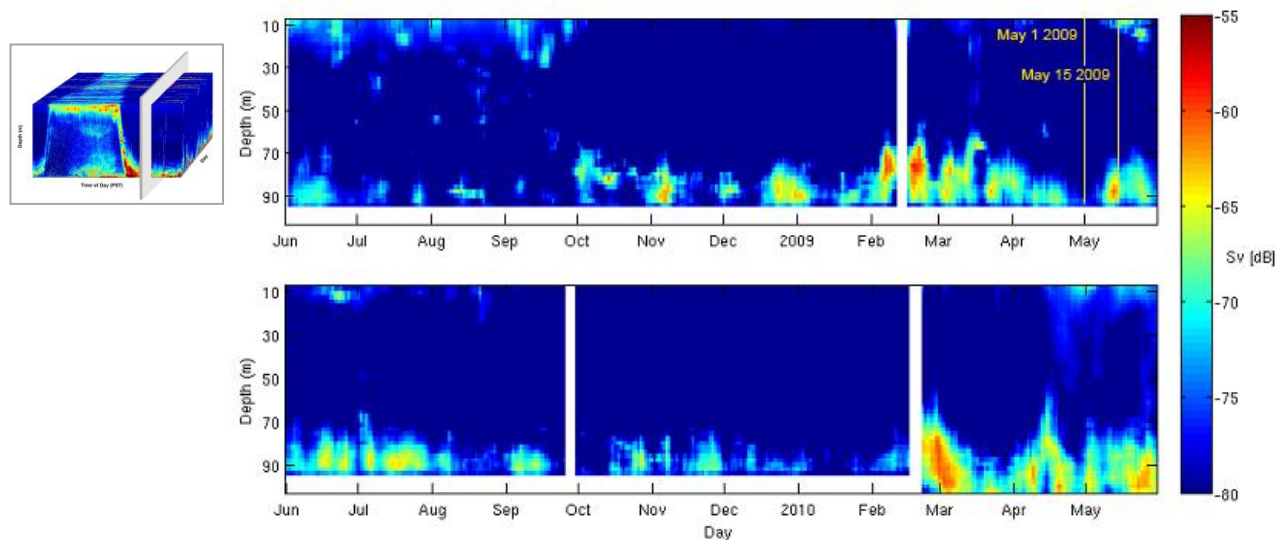
Fig. 3. Echograms of Sv (dB) at noon (12:00 PST) for the period June 1, 2008 – May 31, 2010. A change in recording depth at the end of February 2010 was due to the redeployment of the AWCP at a nearby location but 10 m deeper. The inset illustrates the orientation of the data slice depicted relative to the data cube. High temporal resolution echograms for May 1 and 15, 2009 are shown in Fig 4.

Fig. 3 presents a strongly averaged view of events that does not permit interpretation of the biological communities underlying the signal. Although single frequency sonar data in theory does not support size fractionation of the signal, in fact separation of fish from zooplankton can be inferred from full resolution data based on an interpretation of texture and patterns. The full temporal resolution plots in Fig. 4 show 1 hour of vertical profiles at 3 second intervals, and illustrate the richness of these data. On May 1, 2009, scattering was low throughout the water column. Two weeks later on May 15, strongly scattering shapes appeared in the upper 10m, which may be schools of herring, common in these waters at this time of the year. We have not yet examined other instances of elevated daytime scattering near the surface in Fig. 3, but it seems reasonable to assume that these were caused by fish also. Scattering was low through the rest of the water column, with isolated single, strongly scattering targets appearing below 50 m on May 15. Features that are angled upward to the right in Fig. 4 indicate targets that were moving upwards, and similarly for downward moving targets. These are likely single fish, and appear to be associated with the upper boundary of the deep scattering layer interpreted as zooplankton.
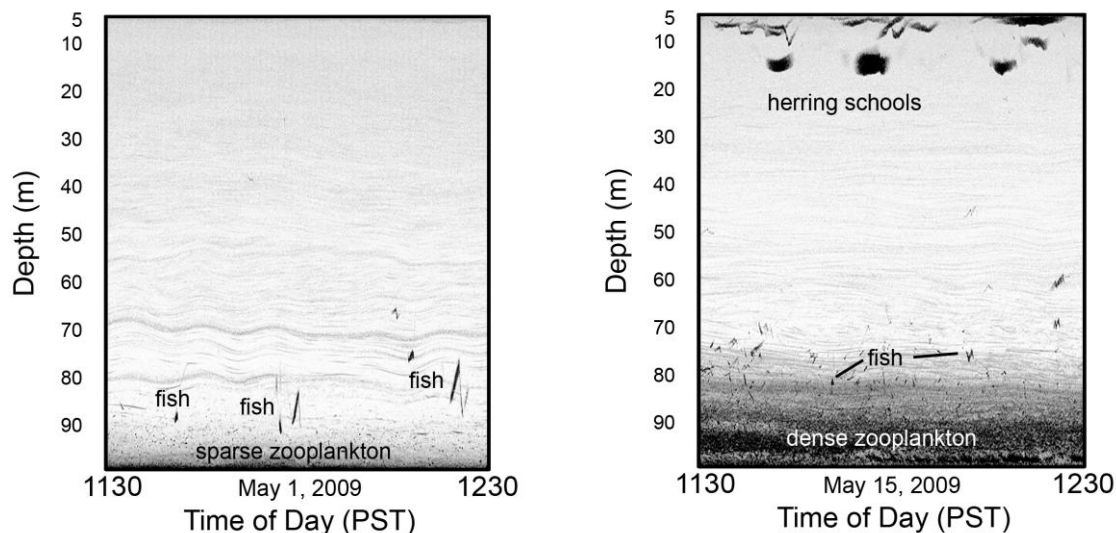

Fig. 4. High temporal resolution plots around noon on May 1 and 15, 2009, illustrating the differences captured in the plot in Fig. 3.

Presented at the Oceans 2010 MTS/IEEE conference, Seattle, Washington, September 20-23, 2010
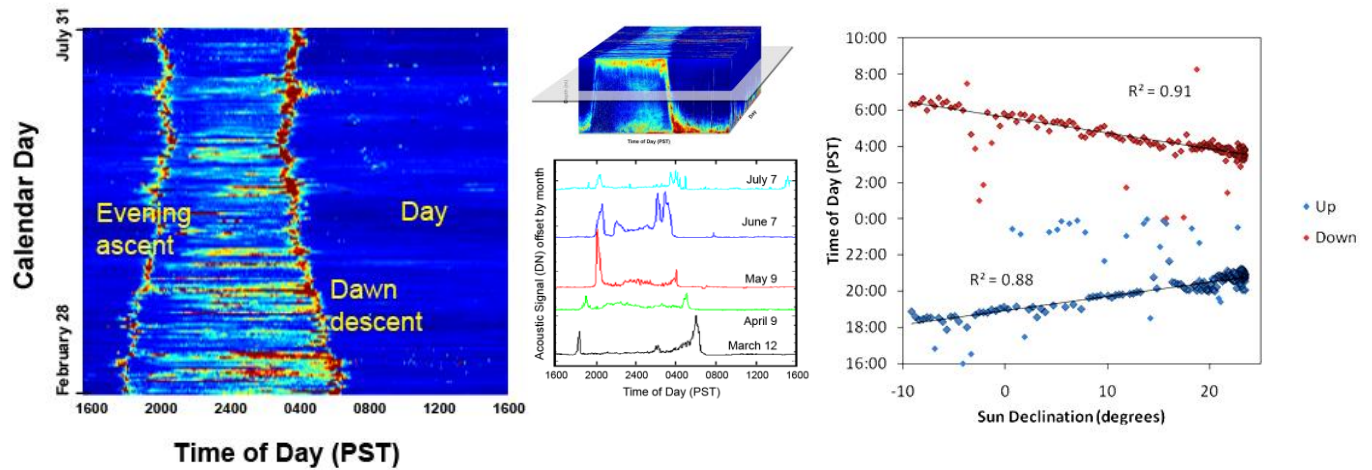
Fig. 5. Left panel: Five months (February 29 - July 31, 2009) of daily, uncalibrated acoustic signal, averaged over the depth interval 39 - 41m to show temporal variation of the diel vertical migrations. Color scale increases from blue (low signal) to red (high signal). Top center figure illustrates the orientation of the data slice depicted relative to the data cube. Bottom center: X profiles across the left panel at the times of the full moons. Right panel: The timing of maximum signal return at 40 m for the ascent and descent, plotted versus solar declination.

B   Timing of the diel vertical migration

The strongest signal in the data is that of the Diel Vertical Migration (DVM). The exact timing of initiation of both the upward and downward migrations is not always clear, but simple horizontal slices through the data cube at mid-depth can be used to describe the timing of the migrations (Fig. 5).

The left panel in Fig. 5 illustrates the seasonal variation of the daily timing of average scattering for the depth interval 39 to 41 m, as shown in the center top panel. The lower center graphic shows graphics profiles across the left panel on the full moon of each month (bottom to top: Mar 12, Apr 9, May 9, June 7, July 7), emphasizing the sharp narrow peak in scattering as the zooplankton moved through the 40 m depth. The right panel in Fig. 5 plots the timing of the upward evening ascent and the downward dawn descent (defined here simply as the timing of the maximum scattering at 40 m during the dusk and dawn periods) versus sun declination, emphasizing the very close relationship with daylength.

Variations in the timing of the DVM can be qualitatively recognized in the left panel of Fig. 5 as 'flares' or deviations from the sinusoidal curves representing the evening ascent and the dawn descent. Because of the simple 'maximum scattering at one-depth' method of calculating the timing of the DVM, our calculation is noisy and susceptible to strong signals from fish, for example. A least squares fit through many depths on each day would provide a more robust estimate. Fig. 6 gives a time series of migration timing anomalies based on deviations from the relationship with sun declination from Fig. 5. In order to evaluate the extent to which these deviations were attributable to false signals from fish, versus true variations in DVM timing, we examined the full temporal resolution data for the dates indicated by the colored circles in Fig. 6.
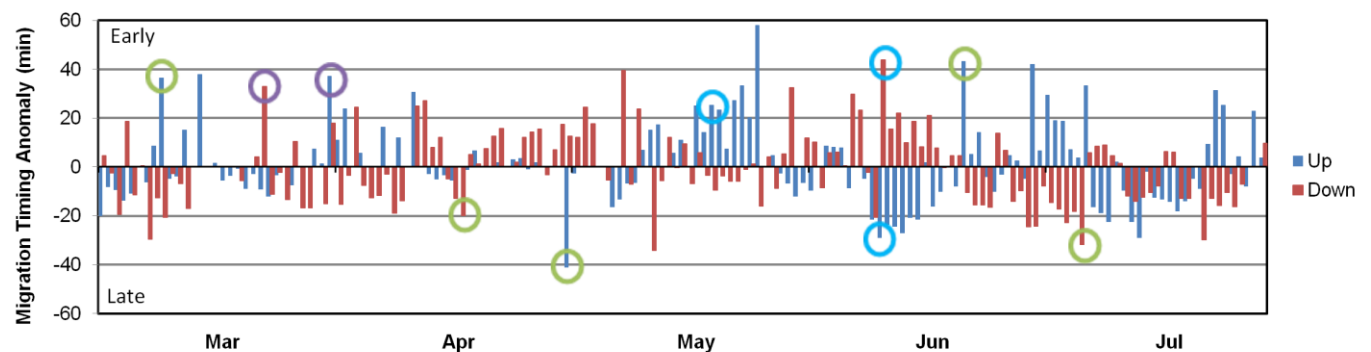

Fig. 6. Vertical migration timing anomalies for the period February 28 to July 31, 2009, where anomalies were calculated relative to the relationship with sun declination as shown in Fig 5. Circles illustrate migration events that were examined in more detail using the high temporal resolution data. Circle colors reflect the major cause for the anomaly in each case (see Table 2).
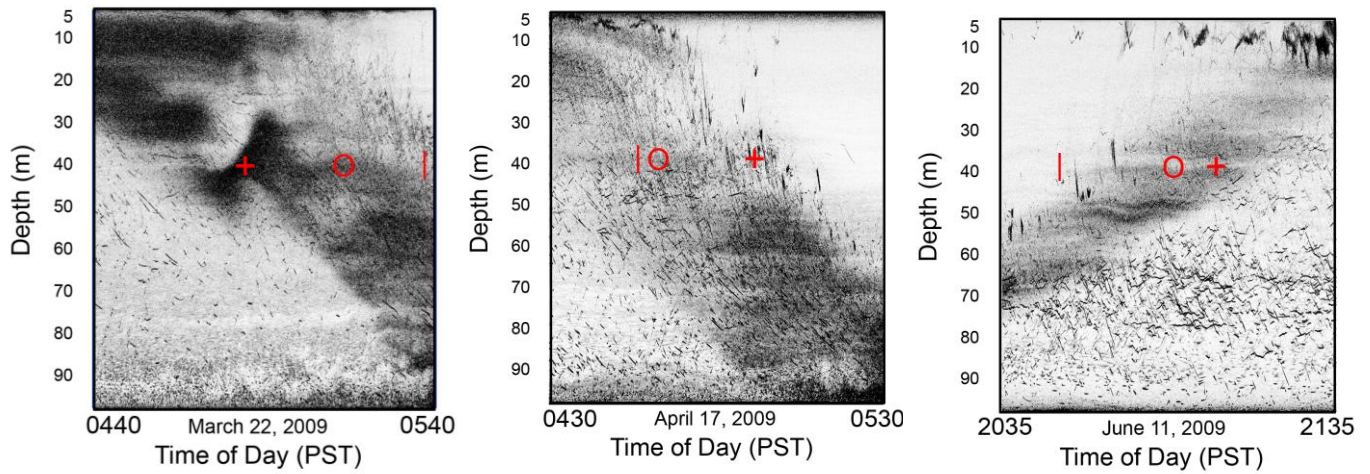
Fig. 7. One hour high-temporal resolution time series on three days, to illustrate three different causes of anomalies seen in Fig. 6. On March 22 internal waves disrupted the downward migration. On April 17 fish following the downward migration interfered with the algorithm. On June 11 the anomaly reflects a real delay in migration timing. In each case, the vertical line indicates the expected timing at 40m; the cross indicates the timing found by the simple maximum algorithm. The approximate timing of each migration selected manually is shown by an open circle.

An examination of the data in Fig. 7 shows examples of three sources of timing anomalies. The March 22 image seems to show the passage of an internal wave though the migrating layer. The April 17 image shows an instance of an error resulting from a fish target located near the margin of the zooplankton layer (+). The manually selected timing estimate (o) shows that the migration was in fact close to the expected timing (|). The June 11 image shows an example of a real delay in the migration relative to the expected timing. Table 2 summarizes the causes found to be underlying each of the anomalies indicated by the circles in Fig. 6.

TABLE 2
A PARTIAL EXAMINATION OF THE CAUSES OF APPARENT TIMING ANOMALIES IN FIGURE 6.

Date	Observed anomaly	Explanation	Expected (|)	Observed (+)	Corrected time (o)	Corrected anomaly
Mar 9	up 36min early	school of fish	18:29	17:53	18:29	00:00
Mar 22	down 33min early	physical disruption of the zooplankton layer, early migration	5:40	5:08	05:24	00:16 early
Mar 31	up 37min early	physical disruption of the zooplankton layer, early migration	19:11	18:34	18:35	00:36 early
Apr 17	down 20min late	individual fish	4:47	5:07	4:49	00:02 late
May 1	up 41 min late	Zooplankton very sparse, algorithm found a fish, migration slightly early	20:04	20:46	19:53	00:11 early
May 20	up 25 min early	migration early	20:29	20:04	20:00	00:29 early
June 11	down 44 min early	fish within zooplankton layer, migration early	3:36	2:53	3:01	00:35 early
June 11	up 24 min late	migration late	20:45	21:14	21:05	00:20 late
June 22	up 43 min early	dense school of fish	20:47	20:04	20:49	00:02 late
July 7	down 32 min late	school of fish	03:38	04:10	03:45	00:07 late

I. DISCUSSION

As expected, our analysis of the long AWCP time series, which is just beginning, is showing evidence of seasonal cycles (Fig. 3). Two years of continuous acoustic observations in Saanich Inlet show the seasonal changes in the daytime scattering layer. The weak scattering layer periodically observed in Fig. 3 can be due to an absence of zooplankton or a deepening of the scattering layer below the instrument. The VENUS AWCP is located at 95 m depth on the slope of the deep basin, where maximum depths reach 236 m. Repeated daytime acoustic surveys throughout the inlet using a downward looking 200-kHz AWCP mounted on a vessel have shown that the deep scattering layer is generally located at 75 – 125 m depth [16]. Some of the scattering layer is therefore located below the instrument during the daytime. In Saanich Inlet, *Euphausia pacifica* is known to be the dominant species comprising the deep scattering layer [15]. Our future analyses will focus on nighttime profiles, when the zooplankton are concentrated near the surface.

Presented at the Oceans 2010 MTS/IEEE conference, Seattle, Washington, September 20-23, 2010

Our analysis in Fig. 5 shows the strong scattering layer ascending at dusk and descending at dawn in Saanich Inlet, in agreement with observations of shorter time series by others [e.g., 13-16]. We have demonstrated that even with very simple algorithms, we can capture the timing of the passage of the scattering layer through the 40 m depth interval, and show a very strong correlation between timing and sun declination in time averaged data (Fig. 6). Using low temporal resolution data or applying temporal averaging can produce spurious anomalies however. Examination of high temporal resolution profiles (Fig. 7) shows that both fish and physics in the form of internal waves can cause errors in the interpretation of the signal. More intelligent algorithms that exploit the high temporal resoludion of the AWCP are required.

Even with the instrument set up to measure volume backscatter, fish targets are commonly seen in throughout the water column - both as individual targets, and as schools (Fig.7). The long time series is a rich source of behavioral data for both fish and zooplankton, and their interactions. We commonly see fish targets mingling with and following the more diffuse zooplankton scattering clouds in time and space, suggesting feeding by the fish on the zooplankton. Reference [16] had insufficient data to determine whether fish were descending with zooplankton or whether the schools were waiting near the bottom. We see examples of both behaviors. The center panel of Fig. 7 is a particularly good example of fish following the downward migration, even changing their swimming speed and direction to match that of the zooplankton. We have not yet carefully analyzed the data looking at the fish targets, but we see many examples of zooplankton distribution influencing fish, as well as occasions when fish influenced the distribution of zooplankton.

REFERENCES

[1]   C. N. Flagg and S. L. Smith. 1989. On the use of the acoustic Doppler current profiler to measure zooplankton abundance. Deep Sea Res. 36: 455-474.
[2]   R. E. Thomson and S. E. Allen. 2000. Time series acoustic observation of macrozooplankton diel migration and associated pelagic fish abundance. Can. J. Fish. Aquatic Sci. 57:1919-1931.
[3]   D. D. Lemon, R. A. Chave, M. R. Clarke, R. K. Dewey and P. Macoun. "Inverted Echo Sounder on a Cabled Observatory". *Proc. MTS/IEEE International Conf. Oceans 2007*, October, 2007
[4]   D. D. Lemon, d. Billenness and J. Buermans. " Comparison of Acoustic Measurements of Zooplankton Populations Using an Acoustic Water Column Profiler and an ADCP". *Proc. MTS/IEEE International Conf. Oceans 2008*, September, 2008.
[5]   R. Dewey, V. Tunnicliffe, and A. Round, "The VENUS Cabled Observatory: An Underview of Engineering Meets Science.", *Proc. MTS/IEEE International Conf. Oceans 2007*, October, 2007
[6]   J. J. Faran, 1951. Sound scattering by solid cylinders and spheres. J. Acoust. Soc. Am. 23: 405-418.
[7]   K. G. Foote, 1982. Optimizing copper spheres for precision calibration of hydroacoustic equipment. J. Acoust. Soc. Am. 71: 742-747.
[8]   R. Hickling, 1962. Analysis of echoes from a solid elastic sphere in water. J. Acoust. Soc. Am. 34: 1582-1592.
[9]   A. A. Proctor, C. Bradley, E. Gamroth and J. Kennedy. 2007. The Ocean Technology Test Bes - An Underwater Laboratory. *Proc. MTS/IEEE International Conf. Oceans 2007*, October, 2007
[10] S. Vagle, K. G. Foote, M. V. Trevorrow and D. M. Farmer. 1996. A technique for calibration of monostatic echosounder systems. IEEE J. Oceanic Eng. 21(3):298-305.
[11] J. J. Anderson and A. H. Devol, 1973. "Deep water renewal in Saanich Inlet, and intermittently anoxic basin". *Estuar. Coast. Mar. Sci.* 1:1-10.
[12] M. Takahashi, D. L. Siebert and W. H. Thomas, 1977. Occasional blooms of phytoplankton during the summer in Saanich Inlet, BC., Canada. Deep Sea Res., 24:775-780.
[13] B. M. Bary, W. E. Barracough and R. Herlineaux. 1962. Scattering of underwater sound in Saanich Inlet, British Columbia. Nature, 194: 36-37.
[14] W. A. Heath, 1977. "The Ecology and Harvesting of Euphausiids in the Strait of Georgia". Ph.D. Thesis, University of British Columbia, Vancouver, Canada.
[15] A. De Robertis 2002. Small scale spatial distribution of the euphausiid *Euphausia pacifica* and overlap with planktivorous fishes. J. Plankton Research, 24:1207-1120.
[16] I. A. Beveridge, 2007. "Acoustic observations of zooplankton distribution in Saanich Inlet, an intermittently anoxic fjord". M.Sc. Thesis, University of Victoria, Canada. Accessed online at http://hdl.handle.net/1828/2287